

## ELECTRODIFFUSIVE FLUX THROUGH A STOCHASTICALLY GATED ION CHANNEL\*

SEAN D. LAWLEY<sup>†</sup> AND JAMES P. KEENER<sup>‡</sup>

**Abstract.** A fundamental assumption of the Hodgkin–Huxley model and other conductance-based neuron models is that the average flux of ions through a stochastically gated ion channel is the product of (a) the flux of ions through a channel that is always open and (b) the proportion of time that the gated channel is open. In this paper, we propose and analyze a model of electrodiffusion through a stochastically gated ion channel to investigate the validity of this classical assumption. We find that this assumption is valid for typical physiological parameter regimes, and we also show that it breaks down for parameters outside of typical physiological ranges. Indeed, we show that the flux through a gated channel can be orders of magnitude larger than this classical assumption if either the gating is fast or the potential difference across the membrane is large. Mathematically, our model consists of one-dimensional advection-diffusion equations with a stochastically switching boundary condition. Employing an iterated random function approach, we prove that the solution converges in distribution at large time and find (i) the support of the solution, (ii) analytical formulas for the mean solution and mean flux, and (iii) analytical formulas for the full probability distribution of the solution in various parameter regimes. All of our analysis is accompanied by numerical simulations of the stochastic PDE.

**Key words.** conductance-based neuron model, random PDE, piecewise deterministic Markov process, stochastic hybrid system, random switching

**AMS subject classifications.** 92C30, 60H15, 35R60, 37H99, 92C20

**DOI.** 10.1137/18M1185041

**1. Introduction.** The Hodgkin–Huxley model [13] is perhaps the most important model in all of physiology. Named after Alan Hodgkin and Andrew Huxley, this mathematical model consists of a system of nonlinear differential equations and describes how action potentials in neurons are initiated and propagated. In addition to transforming the field of neuroscience [11, 24] (Hodgkin and Huxley won the 1963 Nobel Prize in Physiology or Medicine), the model has stimulated an enormous amount of research in mathematics [9].

A fundamental assumption of the Hodgkin–Huxley model and other conductance-based neuron models is that the flux of ions through a stochastically gated ion channel is the product of (a) the flux of ions through a channel that is always open and (b) the proportion of time that the gated channel is open. That is, these models assume

$$(1) \quad J_{\text{gated}} = \rho_0 J_{\text{open}},$$

where  $J_{\text{gated}}, J_{\text{open}}$  are the fluxes through either a gated or always open channel, and  $\rho_0 \in (0, 1)$  is the proportion of time that the gated channel is open. While this assumption is intuitive, to our knowledge, its validity has not been systematically

---

\*Received by the editors May 7, 2018; accepted for publication (in revised form) February 8, 2019; published electronically April 2, 2019.

<http://www.siam.org/journals/siap/79-2/M118504.html>

**Funding:** The work of the first author was supported by NSF grants DMS-RTG 1148230 and DMS-1814832. The work of the second author was supported by NSF grants DMS-RTG 1148230 and DMS 1515130.

<sup>†</sup>Department of Mathematics, University of Utah, Salt Lake City, UT 84112 (lawley@math.utah.edu).

<sup>‡</sup>Departments of Mathematics and Bioengineering, University of Utah, Salt Lake City, UT 84112 (keener@math.utah.edu).

investigated. Indeed, there are several outstanding questions. What conditions guarantee that (1) holds? Are there physiologically relevant situations in which (1) breaks down? Can we ever expect  $J_{\text{gated}}$  to be larger (or smaller) than  $\rho_0 J_{\text{open}}$ ? How does the validity of (1) depend on the many parameters involved, such as the electric potential difference across the cell membrane, ion diffusion coefficients, gating rates, etc.?

In this paper, we propose and analyze a model of electrodiffusion through a stochastically gated ion channel to investigate the validity of the classical assumption in (1) and answer these questions. We find that (1) is valid for typical physiological parameter regimes. This agreement is an important validation of our model, since the full Hodgkin–Huxley model quantitatively reproduces a large range of empirical data. However, our analysis predicts that (1) breaks down for parameters not far outside of typical physiological ranges. Indeed, we show that  $J_{\text{gated}}$  can be much higher than  $\rho_0 J_{\text{open}}$  if either (i) the gating is fast or (ii) the potential difference across the membrane is large (in a sense to be made precise below).

Mathematically, our model of ion channel conduction takes the form of advection–diffusion equations on a finite interval with stochastically switching boundary conditions. We employ several methods to analyze this random partial differential equation (PDE). First, we cast the problem in a framework of iterated random functions and prove that the solution converges in distribution at large time. We then determine the support of this large time random solution and find analytical formulas for its probability distribution in various parameter regimes. Following these results about the full distribution of the solution, we derive and analyze analytical formulas for the mean solution and the mean flux at large time. Our analysis is accompanied by numerical simulations of the stochastic PDE.

The diffusion equation on an interval with randomly switching boundary conditions was first studied in [19], and additional methods of analyzing similar stochastic PDEs were then developed in [3, 16]. Closely related models were later studied in the chemical physics literature [1, 2]. Additional related work includes extensions of the classical Smoluchowski theory of diffusion-influenced reactions to stochastically gated reactions [4, 8, 26]. In contrast to previous work, the PDE in this paper includes advection, and we study the full probability distribution of the random solution rather than only the mean.

The rest of the paper is organized as follows. First, we formulate the model and describe our main results in section 2. We then present our mathematical analysis in sections 3–4, with section 3 focusing on the full distribution of the random solution and section 4 focusing on its mean. In section 5, we explore our results for typical physiological parameter values. We conclude with a brief discussion.

## 2. Model and main results.

**2.1. Gate always open.** We first describe an electrodiffusion model for an ion channel that is always open. Generalizing the model in Chapter 3 of [14], we suppose that there are  $N$  types of ions,  $S_1, \dots, S_N$  with concentrations  $\bar{c}_1(\bar{x}, \bar{t}), \dots, \bar{c}_N(\bar{x}, \bar{t})$ , passing through an ion channel of length  $L > 0$ ; see Figure 1. The ion channel is in a cell membrane separating the inside of the cell (at  $\bar{x} = 0$ ) from the outside of the cell (at  $\bar{x} = L$ ).

Denoting the valences of the  $N$  ions by  $z_1, \dots, z_N$ , the potential in the channel  $\bar{\phi}(\bar{x}, \bar{t})$  satisfies Poisson’s equation,

$$(2) \quad \frac{\partial^2}{\partial \bar{x}^2} \bar{\phi} = -\frac{F}{\epsilon'} \sum_{k=1}^N z_k \bar{c}_k,$$

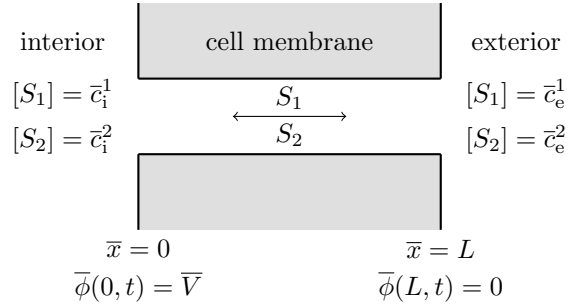


FIG. 1. Schematic diagram of electrodiffusion model for two ions in an ion channel that is always open.

where  $F$  is Faraday's constant and  $\varepsilon'$  is the dielectric constant of the channel medium. The ion concentrations satisfy the conservation equation,

$$\frac{\partial}{\partial t} \bar{c}_k = -\frac{\partial}{\partial x} J_{\text{NP}}^k, \quad k \in \{1, \dots, N\},$$

where the movement of ions in response to a concentration gradient and an electric field is described by the Nernst–Planck equation,

$$(3) \quad J_{\text{NP}}^k = -D_k \left( \frac{\partial}{\partial \bar{x}} \bar{c}_k + \frac{z_k F}{RT} \bar{c}_k \frac{\partial}{\partial \bar{x}} \bar{\phi} \right), \quad k \in \{1, \dots, N\},$$

where  $D_1, \dots, D_N > 0$  are the diffusion coefficients of the  $N$  ions,  $R$  is the universal gas constant, and  $T$  is absolute temperature.

Putting this together, the ion concentrations satisfy the advection-diffusion equations,

$$(4) \quad \frac{\partial}{\partial \bar{t}} \bar{c}_k = D_k \left[ \frac{\partial^2}{\partial \bar{x}^2} \bar{c}_k + \frac{\partial}{\partial \bar{x}} \left( \frac{z_k F}{RT} \bar{c}_k \frac{\partial}{\partial \bar{x}} \bar{\phi} \right) \right], \quad k \in \{1, \dots, N\},$$

where the advection velocity  $\frac{\partial}{\partial \bar{x}} \bar{\phi}$  couples to  $\bar{c}_1, \dots, \bar{c}_N$  through Poisson's equation (2).

Supposing that the ion channel is always open, the boundary conditions are

$$(5) \quad \bar{c}_k(0, \bar{t}) = \bar{c}_1^k > 0, \quad \bar{c}_k(L, \bar{t}) = \bar{c}_e^k > 0, \quad k \in \{1, \dots, N\},$$

$$(6) \quad \bar{\phi}(0, \bar{t}) = \bar{V}, \quad \bar{\phi}(L, \bar{t}) = 0.$$

Here,  $\bar{c}_1^k$  and  $\bar{c}_e^k$  denote the internal and external concentrations of the  $k$ th ion. Further,  $\bar{V}$  is the potential difference across the membrane, defined as the internal potential minus the external potential.

We nondimensionalize by defining new time and space variables,  $t = \frac{D_1}{L^2} \bar{t}$ ,  $x = \bar{x}/L$ , and

$$(7) \quad \phi = \bar{\phi} z_1 F / (RT), \quad V = \bar{V} z_1 F / (RT), \quad c_k = \bar{c}_k / (\bar{c}_e^k + \bar{c}_1^k) \quad \text{for } k \in \{1, \dots, N\},$$

and  $c_1^k = \bar{c}_1^k / (\bar{c}_e^k + \bar{c}_1^k)$ ,  $c_e^k = \bar{c}_e^k / (\bar{c}_e^k + \bar{c}_1^k)$  for  $k \in \{1, \dots, N\}$ . In these new variables, our PDEs (2) and (4) become

$$(8) \quad \frac{\partial}{\partial t} c_k = D_k / D_1 \left[ \frac{\partial^2}{\partial x^2} c_k + \frac{z_k}{z_1} \frac{\partial}{\partial x} \left( c_k \frac{\partial}{\partial x} \phi \right) \right], \quad k \in \{1, \dots, N\},$$

$$(9) \quad \frac{\partial^2}{\partial x^2} \phi = -\sum_{k=1}^N \gamma_k \bar{c}_k,$$

where we have defined the dimensionless constants,

$$\gamma_k = \frac{L^2 F^2 (\bar{c}_e^k + \bar{c}_i^k) z_k}{\varepsilon' R T z_1}, \quad k \in \{1, \dots, N\}.$$

The boundary conditions (5)–(6) become

$$(10) \quad c_k(0, t) = c_i^k \in (0, 1), \quad c_k(1, t) = c_e^k = 1 - c_i^k, \quad k \in \{1, \dots, N\},$$

$$(11) \quad \phi(0, t) = V, \quad \phi(1, t) = 0.$$

Even at steady state, these equations cannot be solved analytically. However, one can find approximate steady state solutions if  $\gamma := \max_k \{|\gamma_k|\} \ll 1$ . In particular, if  $\gamma \ll 1$  (the so-called short channel or low concentration limit), then (9) becomes Laplace's equation  $\frac{\partial^2}{\partial x^2} \phi = 0$ . Hence, upon consulting the boundary conditions for  $\phi$ , we see that the electric potential is the linear function

$$(12) \quad \phi(x, t) = (1 - x)V.$$

It follows that  $c_1, \dots, c_N$  decouple, and (8) becomes the advection-diffusion equation for  $k = 1$ ,

$$(13) \quad \frac{\partial}{\partial t} c = \frac{\partial^2}{\partial x^2} c - V \frac{\partial}{\partial x} c,$$

after dropping the subscript on the ion concentration. Indeed, we henceforth consider only  $c(x, t) := c_1(x, t)$  with boundary conditions  $c(0, t) = c_i := c_i^1$  and  $c(1, t) = c_e := c_e^1$ , since the analysis of  $c_k(x, t)$  is the same after replacing  $V$  by  $(z_k/z_1)V$  and using diffusion coefficient  $D_k/D_1$ .

One can show that the steady state ion concentration  $\lim_{t \rightarrow \infty} c(x, t)$  is

$$(14) \quad u_0^{ss}(x) := \frac{c_i(e^V - e^{Vx}) + c_e(e^{Vx} - 1)}{e^V - 1},$$

and the steady state ion flux is

$$(15) \quad J_{\text{open}} := V \frac{c_i - c_e e^{-V}}{1 - e^{-V}}.$$

Equation (15) is the famous Goldman–Hodgkin–Katz flux equation and is commonly used in models of cellular electrical activity [12].

**2.2. Stochastic gating.** We now modify this classical electrodiffusion model by supposing that the channel is gated. Specifically, we suppose that the channel has a gate at  $x = 1$  that opens and closes according to a two-state Markov jump process  $n(t) \in \{0, 1\}$  with dimensionless transition rates  $\alpha_0 > 0, \alpha_1 > 0$ ,

$$(16) \quad \text{open} \quad 0 \xrightleftharpoons[\alpha_1]{\alpha_0} 1 \quad \text{closed}.$$

Of course, if the dimensional rates are  $\bar{\alpha}_0, \bar{\alpha}_1$ , then  $\alpha_0 = \frac{L^2}{D_1} \bar{\alpha}_0$  and  $\alpha_1 = \frac{L^2}{D_1} \bar{\alpha}_1$ . We have assumed a two-state channel for simplicity, though we note that more complex gating models involving multiple subunits of multiple types are commonly used [5, 10, 14] (see the discussion section below for more on this topic).

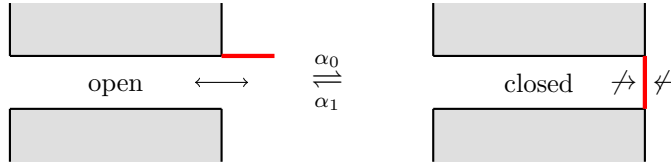


FIG. 2. Schematic diagram of electrodiffusion model in a stochastically gated ion channel.

We model the effect of the gate by making the boundary condition for  $c$  at  $x = 1$  depend on the state of the gate. In particular, when the gate is open ( $n(t) = 0$ ), then we impose

$$(17) \quad c(1, t) = c_e,$$

and when the gate is closed ( $n(t) = 1$ ), we impose

$$(18) \quad \frac{\partial}{\partial x} c(1, t) - Vc(1, t) = 0.$$

That is, we impose the condition in (10) when the gate is open, and we impose a no flux condition when the gate is closed; see Figure 2. The boundary condition for  $c$  at  $x = 0$  is unchanged and is independent of the gate,

$$(19) \quad c(0, t) = c_i.$$

Since the gate  $n(t)$  is a stochastic process, it follows that  $\{c(x, t)\}_{t \geq 0}$  is now a stochastic process.

In this paper, we investigate how the stochastic opening and closing of the gate affects the ionic flux. It is commonly assumed [12] that the flux through a gated channel is merely the flux through an always open channel multiplied by the proportion of time that the gated channel is open. For our model of a gate (16), this means that

$$(20) \quad J_{\text{gated}} = \rho_0 J_{\text{open}},$$

where  $J_{\text{gated}}, J_{\text{open}}$  are the fluxes through either a gated or always open channel, and  $\rho_0 := \frac{\alpha_1}{\alpha_1 + \alpha_0} \in (0, 1)$  is the proportion of time that the gated channel is open.

We prove that  $J_{\text{gated}} > \rho_0 J_{\text{open}}$  for all parameter values and that (20) holds only in the limit of either (i) slow gating or (ii) a large negative potential difference. That is, we prove that (20) holds only in the limit of either

$$\alpha_0 + \alpha_1 \rightarrow 0 \quad \text{or} \quad V \rightarrow -\infty.$$

Furthermore, we find an analytical formula for the mean flux through a gated channel that holds for any choice of parameters,  $\alpha_0, \alpha_1, V, c_i$ . This calculation shows that the flux through a gated channel can be much larger than the estimate (20). Indeed, for any fixed proportion of time open  $\rho_0 \in (0, 1)$ , the flux through a gated channel in the fast gating limit is

$$(21) \quad \lim_{\alpha_0 + \alpha_1 \rightarrow \infty} J_{\text{gated}} = J_{\text{open}},$$

where  $J_{\text{open}}$  is given in (15). In addition, for any fixed transition rates  $\alpha_0 > 0, \alpha_1 > 0$ , the flux through a gated channel in the limit of a large potential difference is

$$(22) \quad \lim_{V \rightarrow \infty} J_{\text{gated}} = J_{\text{open}}.$$

**3. Distribution of the random ion concentration.** In this section, we construct the random solution to (13), (17)–(19) and study its distribution. In particular, we prove that the random solution converges in distribution at large time to an  $L^2[0, 1]$ -valued random function  $C(x)$  and determine the support of  $C(x)$ . We also find analytical formulas for the random function  $C(x)$  in certain parameter limits ( $\alpha_0 + \alpha_1 \rightarrow 0$  and  $V \rightarrow \pm\infty$ ).

**3.1. Construction of the random solution.** We first construct the random solution to (13) with boundary condition (19) at  $x = 0$  and randomly switching conditions (17) and (18) at  $x = 1$  by repeatedly composing the solution operators to the pair of deterministic PDEs corresponding to either an open or closed gate. These solution operators are given in the next lemma. In the following, we denote the standard  $L^1[0, 1]$  and  $L^\infty[0, 1]$  norms by  $\|\cdot\|_1$  and  $\|\cdot\|_\infty$ , respectively. We also use the weighted  $L^2[0, 1]$  inner product,

$$(23) \quad (f, g)_w := \int_0^1 f(x)g(x)e^{-Vx} dx,$$

and the associated norm,  $\|f\|_w := \sqrt{(f, f)_w}$ . We note that the spatial differential operators are self-adjoint with this inner product.

LEMMA 3.1. *The solution operator,  $\Phi_0^t : L^2[0, 1] \rightarrow L^2[0, 1]$ , which takes an initial condition  $f \in L^2[0, 1]$ , and maps it to the solution of (13) with boundary conditions (17) and (19) is*

$$(24) \quad (\Phi_0^t(f))(x) := u_0^{ss}(x) + \sum_{k=1}^\infty e^{-\mu_0^{(k)}t} (\phi_0^{(k)}, f - u_0^{ss})_w \phi_0^{(k)}(x),$$

where  $u_0^{ss}(x)$  is the steady state solution defined in (14), and the eigenvalues and orthonormal (with respect to  $(\cdot, \cdot)_w$ ) eigenfunctions are

$$-\mu_0^{(k)} := -\left(\frac{V^2}{4} + \lambda_0^{(k)}\right) < 0, \quad \phi_0^{(k)}(x) := \sqrt{2}e^{\frac{V}{2}x} \sin(k\pi x), \quad k \geq 1,$$

where  $\lambda_0^{(k)} := k^2\pi^2 > 0$ .

Similarly, the solution operator of (13) with boundary conditions (18) and (19) is

$$(25) \quad (\Phi_1^t(f))(x) := u_1^{ss}(x) + \sum_{k=0}^\infty e^{-\mu_1^{(k)}t} (\phi_k, f - u_1^{ss})_w \phi_1^{(k)}(x),$$

where  $u_1^{ss}(x) := c_1e^{Vx}$ , and the eigenvalues are  $-\mu_1^{(k)} := -\left(\frac{V^2}{4} + \lambda_1^{(k)}\right) < 0$  for  $k \geq 1$ , where  $\{\lambda_1^{(k)}\}_{k=1}^\infty$  are the positive solutions of the transcendental equation

$$\frac{\tan(\sqrt{\lambda})}{\sqrt{\lambda}} = \frac{2}{V},$$

and the associated eigenfunctions are  $\phi_1^{(k)}(x) := \nu^{(k)}e^{\frac{V}{2}x} \sin(\sqrt{\lambda_1^{(k)}}x)$  for  $k \geq 1$ , where  $\nu^{(k)}$  is such that  $\|\phi_1^{(k)}\|_w = 1$ . If  $V \leq 2$ , then  $\phi_1^{(0)} \equiv 0$  and the value of  $\mu_1^{(0)}$  is

irrelevant. If  $V > 2$ , then  $-\mu_1^{(0)} := -(\frac{V^2}{4} + \lambda_1^{(0)}) < 0$ , where  $\lambda_1^{(0)} \in (-\frac{V^2}{4}, 0)$  is the unique solution of the transcendental equation

$$(26) \quad \frac{\tanh(\sqrt{-\lambda_0})}{\sqrt{-\lambda_0}} = \frac{2}{V},$$

and  $\phi_1^{(0)}(x) := \nu^{(0)} e^{\frac{V}{2}x} \sin(\sqrt{\lambda_1^{(0)}}x)$ , where  $\nu^{(0)}$  is such that  $\|\phi_1^{(0)}\|_w = 1$ .

As the operators involved are self-adjoint, the proof of Lemma 3.1 is straightforward and is therefore omitted.

Having defined the maps  $\Phi_0^t$  and  $\Phi_1^t$ , the solution of (13) with randomly switching boundary conditions (17)–(18) is constructed by iteratively composing these maps according to the transition times of the Markov process  $\{n(t)\}_{t \geq 0}$ . More precisely, let  $\{\xi_k\}_{k=1}^\infty$  denote the sequence of states visited by  $\{n(t)\}_{t \geq 0}$ . That is, let  $\xi_1 \in \{0, 1\}$  be a Bernoulli random variable with mean  $\rho_0 = \frac{\alpha_1}{\alpha_0 + \alpha_1}$  and let  $\xi_k = 1 - \xi_{k \pm 1}$ . Further, let  $\{s_k\}_{k=1}^\infty$  be a sequence of independent exponential random variables, each with mean  $\mathbb{E}[s_k] = 1$ . The sequence of sojourn times of  $\{n(t)\}_{t \geq 0}$  are then  $\tau_k := s_k / \alpha_{\xi_k}$  for  $k \geq 1$ , and the time of the  $k$ th switch is

$$S_k := \sum_{j=1}^k \tau_j.$$

Let  $N(t)$  be the number of jumps of  $n$  before time  $t$ ,

$$N(t) := \sup \{k \in \mathbb{N} \cup \{0\} : S_k < t\},$$

and let  $a(t) := t - S_{N(t)}$  be the time elapsed since the last jump. The random solution at time  $t \geq 0$  is then

$$(27) \quad c(x, t) = \Phi_{\xi_{N(t)+1}}^{a(t)} \circ \Phi_{\xi_{N(t)}}^{S_{N(t)}} \circ \dots \circ \Phi_{\xi_1}^{S_1}(c(x, 0)).$$

**3.2. Large time distribution of random solution.** To prove that  $c(x, t)$  converges in distribution at large time and to study this limiting distribution, we apply the methods developed in [19]. In order to apply these methods, we need to check that the maps  $\Phi_0^t, \Phi_1^t$  in (27) are contracting on average, which we prove in the following lemma.

LEMMA 3.2. *For each  $n \in \{0, 1\}$ , there exists a constant  $\zeta_n > 0$  so that for all  $f, g \in L^2[0, 1]$  and  $t \geq 0$ , we have that*

$$\|\Phi_n^t(f) - \Phi_n^t(g)\|_w \leq e^{-\zeta_n t} \|f - g\|_w.$$

*Proof.* Since  $\mu_0^{(k)} > 0$  for  $k \geq 1$ , we have that

$$(28) \quad \begin{aligned} \|\Phi_0^t(f) - \Phi_0^t(g)\|_w^2 &= \left\| \sum_{k=1}^\infty e^{-\mu_0^{(k)} t} (\phi_0^{(k)}, f - g)_w \phi_0^{(k)} \right\|_w^2 \\ &= \sum_{k=1}^\infty e^{-2\mu_0^{(k)} t} (\phi_0^{(k)}, f - g)_w^2 \\ &\leq e^{-2\mu_0^{(1)} t} \sum_{k=1}^\infty (\phi_0^{(k)}, f - g)_w^2 = e^{-2\mu_0^{(1)} t} \|f - g\|_w^2. \end{aligned}$$

Thus, we may take  $\zeta_0 = \mu_0^{(1)} > 0$ . Taking either  $\zeta_1 = \mu_1^{(1)} > 0$  for  $V \leq 2$  or  $\zeta_1 = \mu_1^{(0)} > 0$  for  $V > 2$ , the proof for  $n = 1$  is the same.  $\square$

Having established that the maps  $\Phi_0^t, \Phi_1^t$  are contractions, we can now determine the large time distribution of  $c(x, t)$ . To describe this distribution, we need some more notation. Define the two compositions,

$$\Psi_n^{s,t} = \Phi_n^{s/\alpha_n} \circ \Phi_{1-n}^{t/\alpha_{1-n}}, \quad s, t \geq 0, \quad n \in \{0, 1\},$$

and the two  $L^2[0, 1]$ -valued random variables,

$$(29) \quad C_n := \lim_{K \rightarrow \infty} \Psi_n^{s_1, s_2} \circ \Psi_n^{s_3, s_4} \circ \dots \circ \Psi_n^{s_{2K-1}, s_{2K}}(f), \quad f \in L^2[0, 1], \quad n \in \{0, 1\}.$$

As above,  $\{s_k\}_{k=1}^\infty$  is a sequence of independent exponential random variables, each with mean  $\mathbb{E}[s_k] = 1$ . The random variables  $C_0, C_1$  are called random pullback attractors because they take an initial condition (here,  $f \in L^2[0, 1]$ ) and pull it back to the infinite past [7, 22, 25]. By Lemma 3.2, we have that  $\Psi_n^{s,t}$  is a contraction in  $L^2[0, 1]$  with the weighted norm  $\|\cdot\|_w$  for all  $s, t > 0$ . Thus, we can apply Proposition 2.1 in [19] to conclude that  $C_0, C_1$  exist almost surely as limits in  $L^2[0, 1]$ , where the notion of convergence is with respect to the weighted norm  $\|\cdot\|_w$ , but convergence in this weighted norm is equivalent to convergence in the standard  $L^2[0, 1]$  norm,  $\|\cdot\|_2$ . Further, Proposition 2.1 in [19] yields that  $C_0, C_1$  are independent of  $f$ .

The following proposition gives the large time distribution of  $c(x, t)$ . The proposition follows immediately from Corollary 2.5 in [19].

**PROPOSITION 3.3.** *If  $\eta \in \{0, 1\}$  is a Bernoulli random variable with mean  $\mathbb{E}[\eta] = \rho_1 := \frac{\alpha_0}{\alpha_0 + \alpha_1}$ , then we have the following convergence in distribution as  $t \rightarrow \infty$ ,*

$$(n(t), c(x, t)) \rightarrow_d (\eta, C(x)) \quad \text{as } t \rightarrow \infty,$$

where  $C$  is the following mixture of the pullbacks in (29),

$$C(x) = (1 - \eta)C_0(x) + \eta C_1(x).$$

In words, Proposition 3.3 says that one can sample the large time distribution of  $c(x, t)$  by doing the following. First, flip a coin (with parameter  $\rho_1$ ) to determine if the gate is either open ( $\eta = 0$ ) or closed ( $\eta = 1$ ). If the gate is open, then sample the pullback  $C_0$  and, if the gate is closed, then sample the pullback  $C_1$ . One can thus think of the pullback  $C_0$  (respectively,  $C_1$ ) as the ion concentration profile in the channel conditioned that the gate is open (respectively, closed).

Using Proposition 3.3, we now determine the support of the large time distribution of  $c(x, t)$ . Put simply, the next proposition ensures that the solution is smooth and lies between the two steady states. Indeed, the region between the two steady states serves as a trapping region for the random PDE; see Figure 3.

**PROPOSITION 3.4.** *Define the set of functions*

$$(30) \quad S := \{g \in C^\infty[0, 1] : \min\{u_0^{ss}(x), u_1^{ss}(x)\} \leq g(x) \leq \max\{u_0^{ss}(x), u_1^{ss}(x)\}\}.$$

Then,

$$\Phi_n^t : S \rightarrow S, \quad n \in \{0, 1\}, \quad t \geq 0,$$

and

$$C(x) \in S \quad \text{almost surely.}$$

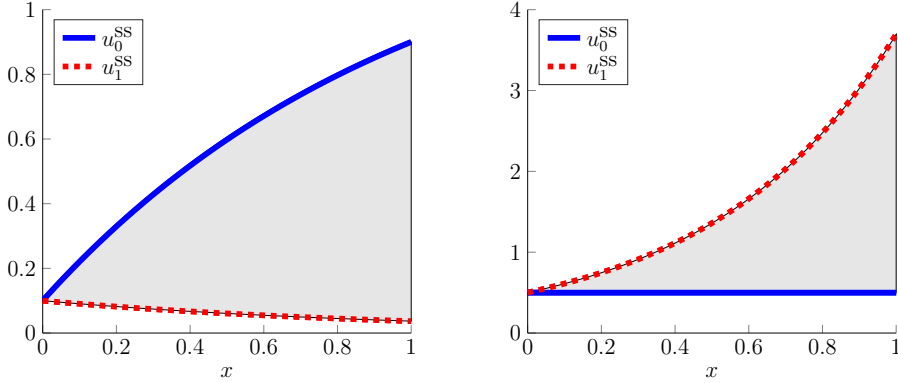


FIG. 3. The support of the large time solution to the random PDE lies between the two steady states,  $u_0^{ss}$  and  $u_1^{ss}$ . Depicted in gray, this trapping region can have either  $u_0^{ss}$  or  $u_1^{ss}$  as its upper or lower boundary, depending on the sign of  $u_0^{ss}(1) - u_1^{ss}(1) = c_e - c_i e^V$ . In the left plot,  $c_i = 0.1$  and  $V = -1$ . In the right plot,  $c_i = 0.5$  and  $V = 2$ .

*Proof.* Let  $g \in S$ . It is immediate that  $\Phi_n^t(g)$  is infinitely differentiable in  $x$  since  $\Phi_n^t(f)$  is infinitely differentiable in  $x$  for each  $f \in L^2[0, 1]$ ,  $t > 0$ .

Defining the ratio  $R(x) = u_0^{ss}(x)/u_1^{ss}(x)$ , a direct calculation shows that

$$\text{sgn}(R'(x)) = \text{sgn}(c_e - c_i e^V) = \text{sgn}(u_0^{ss}(1) - u_1^{ss}(1)), \quad x \in [0, 1],$$

where  $\text{sgn}(z)$  is the signum function. Since  $R(1) = 1$ , it follows that

$$(31) \quad \text{sgn}(u_0^{ss}(x) - u_1^{ss}(x)) = \text{sgn}(u_0^{ss}(1) - u_1^{ss}(1)) = \text{sgn}(c_e - c_i e^V), \quad x \in (0, 1].$$

Suppose  $u_1^{ss}(x) \geq u_0^{ss}(x)$  for some  $x \in (0, 1]$ , thus  $u_1^{ss}(x) \geq u_0^{ss}(x)$  for all  $x \in (0, 1]$  by (31). Observe that

$$\Phi_0^t(g)(x) - \Phi_0^t(u_0^{ss})(x) = \Psi_0^t(g - u_0^{ss})(x),$$

where  $\Psi_0^t$  is the solution operator for the advection-diffusion equation (13) with homogeneous Dirichlet conditions. It is easy to check that  $\Psi_0^t$  satisfies the property that if  $f \geq 0$ , then  $\Psi_0^t(f) \geq 0$ . Therefore, if  $g \in S$ , then  $g(x) - u_0^{ss}(x) \geq 0$  for all  $x \in [0, 1]$ , and thus  $(\Phi_0^t(g))(x) \geq (\Phi_0^t(u_0^{ss}))(x) = u_0^{ss}(x)$  for all  $x \in [0, 1]$  and  $t \geq 0$ .

To check that  $\Phi_0^t(g) \leq u_1^{ss}$ , consider the function

$$h(x, t) := u_1^{ss}(x) - (\Phi_0^t(g))(x).$$

Then,  $h$  satisfies (13) by linearity, with a nonnegative initial condition,  $h(x, 0) = u_1^{ss}(x) - g(x) \geq 0$ , and nonnegative boundary conditions  $h(0, t) = 0$  and  $h(1, t) = u_1^{ss}(1) - c_e \geq 0$ , since  $c_e = u_0^{ss}(1) \leq u_1^{ss}(1)$  by assumption. It follows that  $h(x, t) \geq 0$  for all  $x \in [0, 1]$  and  $t \geq 0$ , and thus  $\Phi_0^t : S \rightarrow S$ . Checking that  $\Phi_1^t : S \rightarrow S$  is similar, and the argument in the case that  $u_1^{ss} \leq u_0^{ss}$  is analogous. Since  $\Phi_n^t : S \rightarrow S$  for  $n \in \{0, 1\}$ , it follows from Theorem 7 on page 24 of [15] that both pullbacks,  $C_0$  and  $C_1$ , are in  $S$ , and thus  $C \in S$ .  $\square$

**3.3. Almost sure limits.** In this section, we use Proposition 3.3 to investigate the ion concentration for either slow gating ( $\alpha_0 + \alpha_1 \ll 1$ ), a large negative potential difference ( $V \ll -1$ ), or a large positive potential difference ( $V \gg 1$ ).

Our first theorem states that the pullbacks defined in (29),  $C_0$  and  $C_1$ , converge to their corresponding steady states solutions,  $u_0^{ss}$  and  $u_1^{ss}$ , in the slow gating limit.

**THEOREM 3.5.** *For any fixed proportion of time open  $\rho_0 \in (0, 1)$  and  $n \in \{0, 1\}$ , we have that*

$$C_n(x) \rightarrow u_n^{ss}(x) \quad \text{uniformly in } x \in [0, 1] \text{ as } \alpha_0 + \alpha_1 \rightarrow 0 \text{ almost surely.}$$

Combining this theorem with Proposition 3.3, it follows that the large time distribution of the random solution in the slow gating limit  $\alpha_0 + \alpha_1 \rightarrow 0$  is

$$(32) \quad (1 - \eta)u_0^{ss}(x) + \eta u_1^{ss}(x),$$

where  $\eta \in \{0, 1\}$  is a Bernoulli random variable with mean  $\mathbb{E}[\eta] = \rho_1 := \frac{\alpha_0}{\alpha_0 + \alpha_1}$ . Having found the entire distribution (32) in this limit, we can of course analytically calculate statistics. For example, the second moment is

$$\mathbb{E} \left[ \{(1 - \eta)u_0^{ss}(x) + \eta u_1^{ss}(x)\}^2 \right] = \rho_0 (u_0^{ss}(x))^2 + \rho_1 (u_1^{ss}(x))^2,$$

and hence the standard deviation is

$$(33) \quad \sqrt{\rho_0 \rho_1} |u_1^{ss}(x) - u_0^{ss}(x)|.$$

*Proof of Theorem 3.5.* As in the definition of  $C_n$  in (29), let  $\{s_k\}_{k=1}^\infty$  be a sequence of independent exponential random variables, each with mean  $\mathbb{E}[s_k] = 1$ . Define the function

$$g_{1-n} := \lim_{K \rightarrow \infty} \Phi_{1-n}^{s_2/\alpha_{1-n}} \circ \Psi_n^{s_3, s_4} \circ \dots \circ \Psi_n^{s_{2K-1}, s_{2K}}(u_0^{ss}).$$

That is,  $g_{1-n}$  is defined so that  $C_n = \Phi_n^{s_1/\alpha_n}(g_{1-n})$ . Since Proposition 3.4 implies that  $g_{1-n} \in S$ , where  $S$  is defined in (30), we have that

$$\begin{aligned} \|C_n - u_n^{ss}\|_\infty &= \|\Phi_n^{s_1/\alpha_n}(g_{1-n}) - u_n^{ss}\|_\infty \\ &\leq e^{-\frac{V^2}{4}s_1/\alpha_n} \sum_k e^{-\lambda_n^{(k)}s_1/\alpha_n} \|(\phi_n^{(k)}, g_{1-n} - u_n^{ss})_w\| \|\phi_n^{(k)}\|_\infty \\ (34) \quad &\leq e^{-\frac{V^2}{4}s_1/\alpha_n} \|u_0^{ss} - u_1^{ss}\|_\infty \sum_k e^{-\lambda_n^{(k)}s_1/\alpha_n} \|e^{-Vx}\phi_n^{(k)}\|_1 \|\phi_n^{(k)}\|_\infty. \end{aligned}$$

Since  $s_1 > 0$  almost surely, taking  $\alpha_0 + \alpha_1 \rightarrow 0$  completes the proof. □

Similarly, our next theorem states that the pullbacks converge to their corresponding steady state solutions in the limit  $V \rightarrow -\infty$ .

**THEOREM 3.6.** *For any fixed proportion of time open  $\rho_0 \in (0, 1)$  and  $n \in \{0, 1\}$ , we have that*

$$|C_n(x) - u_n^{ss}(x)| \rightarrow 0 \quad \text{uniformly in } x \in [0, 1] \text{ as } V \rightarrow -\infty \text{ almost surely.}$$

Combining this theorem with Proposition 3.3, we have that the large time distribution of the random solution in the limit  $V \rightarrow -\infty$  is again given by (32).

*Proof of Theorem 3.6.* As in the proof of Theorem 3.5, we have that for  $V < 2$ ,

$$\|C_n - u_n^{ss}\|_\infty \leq e^{-\frac{V^2}{4}s_1/\alpha_n} \|u_0^{ss} - u_1^{ss}\|_\infty \sum_{k=1}^\infty e^{-\lambda_n^{(k)}s_1/\alpha_n} \|e^{-Vx}\phi_n^{(k)}\|_1 \|\phi_n^{(k)}\|_\infty.$$

It is straightforward to check that if  $V < 0$ , then  $\|u_0^{ss} - u_1^{ss}\|_\infty$ ,  $\|e^{-Vx}\phi_n^{(k)}\|_1$ , and  $\|\phi_n^{(k)}\|_\infty$  can each be bounded above independently of  $V$  and  $k \geq 1$ . Furthermore, it is straightforward to check that for  $V < 0$ , we have

$$-\lambda_1^{(k)} < -(k + 1/2)^2\pi^2 < -k^2\pi^2 = -\lambda_0^{(k)}.$$

Since  $s_1 > 0$  almost surely, taking  $V \rightarrow -\infty$  completes the proof. □

Determining the ion concentration in the limit of a large positive potential difference across the membrane ( $V \gg 1$ ) is more difficult. In particular, we need to control how the principal eigenvalue and eigenfunction associated with  $\Phi_1^t$  behave as  $V$  grows. The first lemma shows that this principal eigenvalue  $-\mu_1^{(0)} = -(\frac{V^2}{4} + \lambda_1^{(0)}) < 0$  vanishes for large  $V$  and bounds the error.

LEMMA 3.7. *For all  $V > 2$ , we have that*

$$(35) \quad 0 < \sqrt{-\lambda_1^{(0)}} = \frac{V}{2} - \frac{V}{1 + e^{2\sqrt{-\lambda_1^{(0)}}}}.$$

Furthermore, for each  $\varepsilon > 0$ , there exists a  $V_0(\varepsilon)$  so that for all  $V \geq V_0(\varepsilon)$  we have that

$$(36) \quad \frac{V}{1 + e^V} < \frac{V}{1 + e^{2\sqrt{-\lambda_1^{(0)}}}} \leq \frac{V}{1 + e^{(1-\varepsilon)V}}.$$

*Proof.* The equality in (35) follows immediately from Lemma 3.1. Since (35) implies  $\sqrt{-\lambda_1^{(0)}} < \frac{V}{2}$ , the first inequality in (36) follows. It follows from (26) that the  $\lim_{V \rightarrow \infty} \sqrt{-\lambda_1^{(0)}} = \infty$ , since  $\lim_{x \rightarrow 0} \tanh(x)/x = 1$ . Thus,  $\lim_{V \rightarrow \infty} \tanh(\sqrt{-\lambda_1^{(0)}}) = 1$  and therefore for each  $\varepsilon > 0$ , we can find  $V_0(\varepsilon)$  so that for all  $V \geq V_0(\varepsilon)$ ,

$$(1 - \varepsilon)V \leq V \tanh(\sqrt{-\lambda_1^{(0)}}) = 2\sqrt{-\lambda_1^{(0)}},$$

by (26). The second inequality in (36) follows. □

The next lemma controls the asymptotic behavior of the principal eigenfunction  $\phi_1^{(0)}$  and related quantities. It is convenient to refer to the normalizing factor in this eigenfunction, so we define  $\psi(x) := e^{\frac{V}{2}x} \sinh(\sqrt{-\lambda_1^{(0)}}x)$  and thus  $\phi_1^{(0)}(x) = \nu_1^{(0)}\psi(x)$ . Further, since  $\lambda_1^{(0)} \approx -\frac{V^2}{4}$  for large  $V$ , we define  $\tilde{\phi} := \tilde{\nu}\tilde{\psi}$ , where

$$\tilde{\psi}(x) = e^{\frac{V}{2}x} \sinh\left(\frac{V}{2}x\right), \quad \tilde{\nu} = \left[\int_0^1 \sinh^2\left(\frac{V}{2}y\right) dy\right]^{-1/2} = \sqrt{\frac{2V}{\sinh(V) - V}}.$$

LEMMA 3.8. *As  $V \rightarrow \infty$ , the following asymptotic behavior holds:*

$$\begin{aligned} (\nu_1^{(0)})^2 &= \mathcal{O}(Ve^{-V}) = \tilde{\nu}^2, & \psi(x) &= \mathcal{O}(e^{Vx}) = \tilde{\psi}(x), \\ (\psi, u_1^{ss} - u_0^{ss})_w &= \mathcal{O}(e^V) = (\tilde{\psi}, u_1^{ss} - u_0^{ss})_w. \end{aligned}$$

*Proof.* It is immediate that  $\tilde{\nu}^2 = \mathcal{O}(Ve^{-V})$ . It then follows from Lemma 3.7 that  $(\nu_1^{(0)})^2 = \mathcal{O}(Ve^{-V})$ . Similarly, it is immediate that  $\tilde{\psi}(x) = \mathcal{O}(e^{Vx})$ . Again, it follows from Lemma 3.7 that  $\psi(x) = \mathcal{O}(e^{Vx})$ . Now, it is easy to check that  $\|(u_1^{ss} - u_0^{ss})e^{-Vy}\|_1 = \mathcal{O}(1)$ . Since  $\psi(x)$  and  $\tilde{\psi}(x)$  are both  $\mathcal{O}(e^{Vx})$ , it follows that both  $(\psi, u_1^{ss} - u_0^{ss})_w$  and  $(\tilde{\psi}, u_1^{ss} - u_0^{ss})_w$  are  $\mathcal{O}(e^V)$ . □

With these lemmas in place, we are now ready to prove that the ion concentration is unaffected by the gate if the potential difference across the membrane is large ( $V \gg 1$ ). That is, if the potential difference is large, then the ion concentration behaves as if the channel is always open. Intuitively, one can understand this result by noting that (a) the relaxation rate of  $\Phi_0^t$  (the solution operator for an open channel) grows like  $\frac{V^2}{4}$  as  $V$  grows, while (b) the relaxation rate of  $\Phi_1^t$  (the solution operator for a closed channel) vanishes as  $V$  grows. Therefore, if  $V \gg 1$ , then the ion concentration rapidly approaches equilibrium when the channel opens, but it hardly changes when the channel closes. The following theorem makes this precise.

**THEOREM 3.9.** *For any proportion of time open  $\rho_0 \in (0, 1)$  and  $x \in [0, 1)$ , we have*

$$|C(x) - u_0^{ss}(x)| \rightarrow 0 \quad \text{almost surely as } V \rightarrow \infty.$$

It is easy to see from (14) that  $u_0^{ss}(x) \rightarrow c_i$  for  $x \in [0, 1)$  as  $V \rightarrow \infty$ , and thus this theorem implies that  $C(x) \rightarrow c_i$  almost surely as  $V \rightarrow \infty$  for  $x \in [0, 1)$ .

*Proof.* Let  $\{s_k\}_{k=1}^\infty$  and  $g_{1-n}$  be as in the proof of Theorem 3.5. By (34), we have

$$\|C_0 - u_0^{ss}\|_\infty \leq e^{-\frac{V^2}{4}s_1/\alpha_0} \|u_0^{ss} - u_1^{ss}\|_\infty \sum_{k=1}^\infty e^{-\lambda_0^{(k)}s_1/\alpha_n} \|e^{-Vx}\phi_0^{(k)}\|_1 \|\phi_0^{(k)}\|_\infty.$$

It is straightforward to check that  $\|u_0^{ss} - u_1^{ss}\|_\infty \leq e^V$  and  $\|e^{-Vx}\phi_0^{(k)}\|_1 \|\phi_0^{(k)}\|_\infty \leq e^V$  for sufficiently large  $V$ . Since  $\lambda_0^{(k)} = k\pi^2$  and  $s_1 > 0$  almost surely, we have that for sufficiently large  $V$ ,

$$(37) \quad \|C_0 - u_0^{ss}\|_\infty \leq e^{-\frac{V^2}{4}s_1/\alpha_0} e^{2V} \sum_{k=1}^\infty e^{-\lambda_0^{(k)}s_1/\alpha_n}.$$

Thus,  $C_0 \rightarrow u_0^{ss}$  almost surely uniformly in  $x \in [0, 1]$  as  $V \rightarrow \infty$ .

We now check the convergence of  $C_1$  as  $V \rightarrow \infty$ . Observe that

$$|C_1(x) - u_0^{ss}(x)| = |(\Phi_1^{s_1/\alpha_1}(g_0))(x) - u_0^{ss}(x)| \leq \mathcal{S}_1(x) + \mathcal{S}_2,$$

where

$$\begin{aligned} \mathcal{S}_1(x) &:= |u_1^{ss}(x) - u_0^{ss}(x) - e^{-(\frac{V^2}{4} + \lambda_1^{(0)})s_1/\alpha_0} (\phi_1^{(0)}, u_1^{ss} - g_0)_w \phi_1^{(0)}(x)|, \\ \mathcal{S}_2 &:= e^{-\frac{V^2}{4}s_1/\alpha_0} \|u_0^{ss} - u_1^{ss}\|_\infty \sum_{k=1}^\infty e^{-\lambda_1^{(k)}s_1/\alpha_0} \|e^{-Vx}\phi_1^{(k)}\|_1 \|\phi_1^{(k)}\|_\infty. \end{aligned}$$

In the rest of the proof, all of the asymptotic  $\mathcal{O}(\cdot)$  statements are in the limit  $V \rightarrow \infty$ . It is straightforward to check that  $\lambda_1^{(k)} > k^2\pi^2$  and  $\|e^{-Vx}\phi_1^{(k)}\|_1 \|\phi_1^{(k)}\|_\infty = \mathcal{O}(e^V)$  for all  $k \geq 1$ . It follows that  $\mathcal{S}_2$  decays to zero almost surely as  $V \rightarrow \infty$ .

We now move to  $\mathcal{S}_1$ . For ease of notation, in the rest of the proof we drop the subscript and superscripts by setting  $\lambda = \lambda_1^{(0)}$ ,  $\phi = \phi_1^{(0)}$ , and  $\nu = \nu_1^{(0)}$ . Recalling the notation of Lemma 3.8, a direct calculation shows that

$$\tilde{\nu}^2(\tilde{\psi}, u_0^{ss} - u_1^{ss})_w \tilde{\psi} = u_0^{ss} - u_1^{ss}.$$

Thus, adding terms to and subtracting terms from  $\mathcal{S}_1$  and using the triangle inequality yields

$$\begin{aligned} \mathcal{S}_1(x) &\leq |\tilde{\nu}^2(\tilde{\psi}, u_1^{ss} - u_0^{ss})_w \tilde{\psi}(x) - \tilde{\nu}^2(\psi, u_1^{ss} - u_0^{ss})_w \tilde{\psi}(x)| \\ &\quad + |\tilde{\nu}^2(\psi, u_1^{ss} - u_0^{ss})_w \tilde{\psi}(x) - \tilde{\nu}^2(\psi, u_1^{ss} - u_0^{ss})_w \psi(x)| \\ &\quad + |\tilde{\nu}^2(\psi, u_1^{ss} - u_0^{ss})_w \psi(x) - \nu^2(\psi, u_1^{ss} - u_0^{ss})_w \psi(x)| \\ &\quad + |\nu^2(\psi, u_1^{ss} - u_0^{ss})_w \psi(x) - e^{-(\frac{V^2}{4} + \lambda_0)s_1/\alpha_0} \nu^2(\psi, u_1^{ss} - u_0^{ss})_w \psi(x)| \\ &\quad + |e^{-(\frac{V^2}{4} + \lambda_0)s_1/\alpha_0} \nu^2(\psi, u_1^{ss} - u_0^{ss})_w \psi(x) - e^{-(\frac{V^2}{4} + \lambda_0)s_1/\alpha_0} \nu^2(\psi, u_1^{ss} - g_0)_w \psi(x)| \\ &=: \mathcal{T}_1(x) + \mathcal{T}_2(x) + \mathcal{T}_3(x) + \mathcal{T}_4(x) + \mathcal{T}_5(x). \end{aligned}$$

We work on these five terms separately.

Starting with  $\mathcal{T}_1$ , observe that

$$|(\tilde{\psi}, u_1^{ss} - u_0^{ss})_w - (\psi, u_1^{ss} - u_0^{ss})_w| \leq \|(u_1^{ss} - u_0^{ss})e^{-Vy}\|_1 \|\tilde{\psi} - \psi\|_\infty.$$

It is straightforward to check that  $\|(u_1^{ss} - u_0^{ss})e^{-Vy}\|_1 = \mathcal{O}(1)$ . Fix  $x \in [0, 1]$  and choose  $\varepsilon > 0$  so that

$$(38) \quad 0 \leq x < 1 - \varepsilon < 1.$$

If we define

$$E := \frac{V}{1 + e^{2\sqrt{-\lambda_0}^1}},$$

then it follows from Lemma 3.7 and the bound

$$(39) \quad 1 - e^{-y} \leq y, \quad y \in \mathbb{R},$$

that we have

$$(40) \quad \tilde{\psi}(z) - \psi(z) \sim \frac{1}{2}e^{Vz}(1 - e^{-Ez}) = \mathcal{O}(Ve^{Vz}e^{-(1-\varepsilon)V}), \quad z \in [0, 1].$$

Therefore  $\|\tilde{\psi} - \psi\|_\infty = \mathcal{O}(Ve^V e^{-(1-\varepsilon)V})$ . Since  $\tilde{\nu}^2 = \mathcal{O}(Ve^{-V})$  and  $\tilde{\psi}(x) = \mathcal{O}(e^{Vx})$  by Lemma 3.8, and since  $\varepsilon$  satisfies (38), it follows that  $\mathcal{T}_1(x) \rightarrow 0$  almost surely as  $V \rightarrow \infty$ . Similarly, it follows from (40), Lemma 3.8, and (38), that  $\mathcal{T}_2(x) \rightarrow 0$  as  $V \rightarrow \infty$ .

Moving to  $\mathcal{T}_3$ , we first note that

$$\begin{aligned} |\tilde{\nu}^2 - \nu^2| &\leq 2V \left| \frac{\sinh(V - 2E) - \sinh(V) + 2E}{[\sinh(V) - V][\sinh(V - 2E) - (V - 2E)]} \right| \\ &\quad + \left| \frac{4E}{\sinh(V - 2E) - (V - 2E)} \right|. \end{aligned}$$

It follows from Lemma 3.7 that

$$\left| \frac{4E}{\sinh(V - 2E) - (V - 2E)} \right| = \mathcal{O}(Ve^{-(1-\varepsilon)V} e^{-V})$$

and

$$V \left| \frac{E}{[\sinh(V) - V][\sinh(V - 2E) - (V - 2E)]} \right| = \mathcal{O}(Ve^{-(1-\varepsilon)V} e^{-V}).$$

Furthermore, we have that

$$2V \left| \frac{\sinh(V - 2E) - \sinh(V)}{[\sinh(V) - V][\sinh(V - 2E) - (V - 2E)]} \right| \\ \sim V \left| \frac{e^V(e^{-2E} - 1)}{[\sinh(V) - V][\sinh(V - 2E) - (V - 2E)]} \right| = \mathcal{O}(V^2 e^{-(1-\varepsilon)V} e^{-V}),$$

by Lemma 3.7 and (39). Since  $(\psi, u_1^{\text{ss}} - u_0^{\text{ss}})_w = \mathcal{O}(e^V)$  and  $\psi(x) = \mathcal{O}(e^{Vx})$  by Lemma 3.8, and since  $\varepsilon$  satisfies (38), it follows that  $\mathcal{T}_3(x) \rightarrow 0$  almost surely as  $V \rightarrow \infty$ .

Moving to  $\mathcal{T}_4$ , Lemma 3.7 and (39) imply that for sufficiently large  $V$ ,

$$1 - e^{-(\frac{V^2}{4} + \lambda)s_1/\alpha_0} \leq (s_1/\alpha_0)V^2 e^{-(1-\varepsilon)V}.$$

Using Lemma 3.8 and (38), it then follows that  $\mathcal{T}_4(x) \rightarrow 0$  almost surely as  $V \rightarrow \infty$ .

Finally, observe that

$$\mathcal{T}_5(x) = e^{-(\frac{V^2}{4} + \lambda)s_1/\alpha_0} |(\phi, u_0^{\text{ss}} - g_0)_w \phi(x)| \\ \leq e^{-(\frac{V^2}{4} + \lambda)s_1/\alpha_0} \|\phi e^{-Vy}\|_1 \|u_0^{\text{ss}} - g_0\|_\infty \|\phi\|_\infty.$$

It thus follows from (37) and the definition of  $g_0$  that  $\mathcal{T}_5 \rightarrow 0$  almost surely as  $V \rightarrow \infty$ . □

**4. Average ion concentration and ion flux.** The analysis in the previous section allowed us to find analytical formulas for the support of the solution to the random PDE (equations (13), (17)–(19)) and the distribution of the large time solution for slow gating ( $\alpha_0 + \alpha_1 \ll 1$ ) or a large negative or positive potential ( $V \ll -1$  or  $V \gg 1$ ). In this section, we find an analytical formula for the *mean* solution at large time. Hence, this yields information about the solution for any parameter choice (rather than only in certain parameter limits). In addition, it yields the *distribution* of the solution in the limit of fast gating ( $\alpha_0 + \alpha_1 \gg 1$ ).

The first step is to decompose the mean of the solution based on the state of the gate by defining the pair of deterministic functions,

$$w_n(x, t) := \mathbb{E}[c(x, t) 1_{n(t)=n}], \quad n \in \{0, 1\},$$

where  $1_{n(t)=n}$  denotes the indicator function on the event  $n(t) = n$ ,

$$1_{n(t)=n} = \begin{cases} 1 & \text{if } n(t) = n, \\ 0 & \text{otherwise.} \end{cases}$$

Thus,  $\mathbb{E}[c(x, t)] = w_0(x, t) + w_1(x, t)$ . Assuming that

$$\mathbb{E} \sup_{x \in [0, 1]} \left| \frac{\partial}{\partial x} c(x, t) \right| < \infty \quad \text{for each } t \geq 0,$$

it follows from a direct application of Theorem 1 in [16] that  $w_0, w_1$  satisfy the deterministic advection-diffusion-reaction equations,

$$(41) \quad \begin{aligned} \frac{\partial}{\partial t} w_0 &= \frac{\partial^2}{\partial x^2} w_0 - V \frac{\partial}{\partial x} w_0 - \alpha_0 w_0 + \alpha_1 w_1, \\ \frac{\partial}{\partial t} w_1 &= \frac{\partial^2}{\partial x^2} w_1 - V \frac{\partial}{\partial x} w_1 + \alpha_0 w_0 - \alpha_1 w_1. \end{aligned}$$

In words,  $w_n(x, t)$  evolves according to the same advection-diffusion dynamics in (13) plus the switching dynamics (the terms in (41) involving  $\alpha_0, \alpha_1$ ). Furthermore, the boundary conditions are

$$(42) \quad \begin{aligned} w_0(0, t) &= \rho_0 c_i, & w_0(1, t) &= \rho_0 c_e, \\ w_1(0, t) &= \rho_1 c_i, & \frac{\partial}{\partial x} w_1(1, t) - V w_1(1, t) &= 0, \end{aligned}$$

assuming  $n(t)$  starts in its invariant measure,

$$\mathbb{P}(n(0) = 0) = \rho_0 := \frac{\alpha_1}{\alpha_1 + \alpha_0}, \quad \mathbb{P}(n(0) = 1) = \rho_1 := \frac{\alpha_0}{\alpha_1 + \alpha_0}.$$

That is, the conditional expectation,  $\mathbb{E}[c(x, t) | n(t) = n] = w_n(x, t) / \rho_n$  satisfies the boundary condition corresponding to state  $n(t) = n$ .

Adding the PDEs in (41) and taking  $t \rightarrow \infty$  yields that the steady state mean solution is

$$(43) \quad \lim_{t \rightarrow \infty} \mathbb{E}[c(x, t)] = \lim_{t \rightarrow \infty} (w_0(x, t) + w_1(x, t)) = \left( \frac{1 - e^{Vx}}{V} \right) J_{\text{gated}} + c_i e^{Vx},$$

where  $J_{\text{gated}}$  is the flux,

$$-\frac{\partial}{\partial x} (w_0 + w_1) + V (w_0 + w_1),$$

at large time. Solving the boundary value problem (41)–(42) at steady state explicitly, we find that this mean gated flux is

$$(44) \quad J_{\text{gated}} = f(\rho_0, \alpha_0 + \alpha_1, V) J_{\text{open}},$$

where  $J_{\text{open}}$  is the flux when the gate is always open ((15) above), and  $f(\rho_0, \alpha_0 + \alpha_1, V) \in (\rho_0, 1)$  is the dimensionless factor,

$$(45) \quad \begin{aligned} &f(\rho_0, \alpha_0 + \alpha_1, V) \\ &:= \frac{1 - \frac{V/2}{\sqrt{\alpha_0 + \alpha_1 + \frac{V^2}{4}}} \tanh\left(\sqrt{\alpha_0 + \alpha_1 + \frac{V^2}{4}}\right)}{1 - \frac{1}{\rho_0} \left[ 1 - (1 - \rho_0) \coth(V/2) \right] \frac{V/2}{\sqrt{\alpha_0 + \alpha_1 + \frac{V^2}{4}}} \tanh\left(\sqrt{\alpha_0 + \alpha_1 + \frac{V^2}{4}}\right)}, \end{aligned}$$

that describes how gating reduces the flux. Note that since  $f \in (\rho_0, 1)$ , it follows that  $J_{\text{gated}}$  is always strictly larger than the common estimate (20).

**4.1. Limiting behavior of mean solution and flux.** We can now use (43), (44), and (45), to investigate how the mean solution and mean flux behave in various parameter limits.

**4.1.1. Slow gating.** First, it is easy to check that

$$\lim_{\alpha_0 + \alpha_1 \rightarrow 0} f(\rho_0, \alpha_0 + \alpha_1, V) = \rho_0,$$

and thus it follows from (43) and (44) that

$$\lim_{\alpha_0 + \alpha_1 \rightarrow 0} J_{\text{gated}} = \rho_0 J_{\text{open}} \quad \text{and} \quad \lim_{\alpha_0 + \alpha_1 \rightarrow 0} \lim_{t \rightarrow \infty} \mathbb{E}[c(x, t)] = \rho_0 u_0^{\text{ss}}(x) + \rho_1 u_1^{\text{ss}}(x).$$

In words, if the gating is slow, then the gate reduces the flux by the proportion of time that the gate is open. This agrees with Theorem 3.5 above.

**4.1.2. Fast gating.** Next, since  $\lim_{y \rightarrow \infty} \tanh(y)/y = 0$ , it follows that for any  $\rho_0 \in (0, 1]$ ,

$$\lim_{\alpha_0 + \alpha_1 \rightarrow \infty} f(\rho_0, \alpha_0 + \alpha_1, V) = 1.$$

Therefore, it follows from (43) and (44) that in the fast gating limit, the ion flux and ion concentration are as if the gate is always open,

$$(46) \quad \lim_{\alpha_0 + \alpha_1 \rightarrow \infty} J_{\text{gated}} = J_{\text{open}} \quad \text{and} \quad \lim_{\alpha_0 + \alpha_1 \rightarrow \infty} \lim_{t \rightarrow \infty} \mathbb{E}[c(x, t)] = u_0^{\text{ss}}(x).$$

That is, if the gating is fast, then the gate does not affect the ion concentration or ion flux.

While (46) is a result about the large time mean solution, we actually have that the large time variance vanishes in the fast gating limit. The essential idea is that if a random variable  $X \in \mathbb{R}$  satisfies  $X \in [a, b]$  almost surely and  $\mathbb{E}[X] = a$ , then it must be the case that  $X = a$  almost surely. To apply this idea to our situation, we first note that Proposition 3.4 implies that if the solution satisfies

$$(47) \quad \min\{u_0^{\text{ss}}(x), u_1^{\text{ss}}(x)\} \leq c(x, T) \leq \max\{u_0^{\text{ss}}(x), u_1^{\text{ss}}(x)\} \quad \text{for all } x \in [0, 1],$$

at some some  $T > 0$ , then we actually have that the solution satisfies that inequality for all future time  $t \geq T$ ,

$$(48) \quad \min\{u_0^{\text{ss}}(x), u_1^{\text{ss}}(x)\} \leq c(x, t) \leq \max\{u_0^{\text{ss}}(x), u_1^{\text{ss}}(x)\} \quad \text{for all } x \in [0, 1], t \geq T.$$

It is easy to see that regardless of the initial condition, the solution will almost surely satisfy (47) at some finite time  $T$ , and therefore satisfy (48) for all sufficiently large time. Suppose that  $u_1^{\text{ss}}(1) \leq u_0^{\text{ss}}(1)$ , and thus  $u_1^{\text{ss}}(x) \leq u_0^{\text{ss}}(x)$  for all  $x \in [0, 1]$ . Therefore, by (46), Jensen’s inequality, and (48), we have that

$$(u_0^{\text{ss}}(x))^2 = \lim_{\alpha_0 + \alpha_1 \rightarrow \infty} \lim_{t \rightarrow \infty} \left( \mathbb{E}[c(x, t)] \right)^2 \leq \lim_{\alpha_0 + \alpha_1 \rightarrow \infty} \lim_{t \rightarrow \infty} \mathbb{E} \left[ (c(x, t))^2 \right] \leq (u_0^{\text{ss}}(x))^2.$$

Therefore,

$$\lim_{\alpha_0 + \alpha_1 \rightarrow \infty} \lim_{t \rightarrow \infty} \text{Var}(c(x, t)) = \lim_{\alpha_0 + \alpha_1 \rightarrow \infty} \lim_{t \rightarrow \infty} \left( \mathbb{E}[(c(x, t))^2] - (\mathbb{E}[c(x, t)])^2 \right) = 0.$$

To handle the case that  $u_0^{\text{ss}}(1) \leq u_1^{\text{ss}}(1)$ , we apply the same argument to the function  $\tilde{c}(x, t) := u_1^{\text{ss}}(x) - c(x, t) \in [0, u_1^{\text{ss}}(x) - u_0^{\text{ss}}(x)]$ .

**4.1.3. Large negative or large positive potential difference.** Next, it is easy to check that

$$\lim_{V \rightarrow -\infty} f(\rho_0, \alpha_0 + \alpha_1, V) = \rho_0 \quad \text{and} \quad \lim_{V \rightarrow \infty} f(\rho_0, \alpha_0 + \alpha_1, V) = 1.$$

Using (43) and (44), we can find the mean solution or mean flux in these limits, which agrees with Theorems 3.6 and 3.9 above.

**4.1.4. No potential difference: A stochastically gated Ohm’s law.** Finally, if there is no potential difference across the membrane,  $V = 0$ , then the flux across the membrane is driven solely by the concentration difference across the membrane. In particular, if the channel is always open, then the dimensionless flux is simply

$$J_{\text{open}} = c_i - c_e.$$

This is often referred to as the chemical Ohm’s law (see section 2.2.3 in [14]).

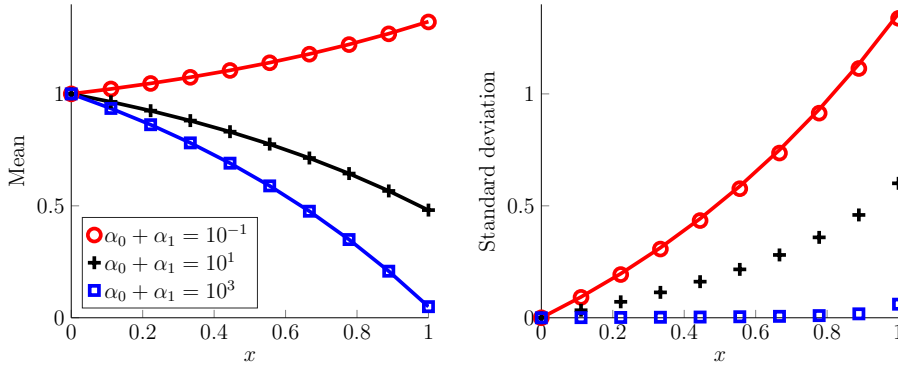


FIG. 4. Pointwise mean and standard deviation of the large time solution of (13), (17)–(19) for different rates of gating,  $\alpha_0 + \alpha_1$ . The markers (circles, plusses, and squares) are results of stochastic simulations of the random PDE. In the left plot, the curves are the analytical formula (43). In the right plot, the red curve is the analytical formula (33), which is valid for slow gating by Theorem 3.5. See section 4.2 for more details.

To find the flux through a gated channel in the absence of a potential difference, we evaluate (44) at  $V = 0$  to obtain

$$(49) \quad J_{\text{gated}} = f(\rho_0, \alpha_0 + \alpha_1, 0)J_{\text{open}} = \left[ 1 + \left( \frac{1 - \rho_0}{\rho_0} \right) \frac{\tanh(\sqrt{\alpha_0 + \alpha_1})}{\sqrt{\alpha_0 + \alpha_1}} \right]^{-1} (c_i - c_e),$$

which recovers a result first found in [19] in a model of insect respiration (see the later works [1, 2] for similar results). We interpret (49) as a stochastically gated chemical Ohm's law. We emphasize that  $f(\rho_0, \alpha_0 + \alpha_1, 0) \rightarrow 1$  as  $\alpha_0 + \alpha_1 \rightarrow \infty$  for each fixed  $\rho_0 \in (0, 1]$ . Thus, even in the purely diffusive case ( $V = 0$ ), the flux through a stochastic gate is the same as if the gate is always open, provided the gating is sufficiently fast.

**4.2. Stochastic simulations.** In Figures 4, 5, and 6, we compare our analytical results with stochastic simulations. To simulate the random PDE system (13), (17)–(19) we first generate a realization of the gate  $n(t)$  until the gate transitions  $10^4$  times. For this realization of the gate, we solve the PDE (13) with alternating boundary conditions (17)–(18) using a MATLAB [21] built-in numerical PDE solver (pdepe) with 100 spatial grid points. We then sample the solution at the  $10^4$  switching times to compute statistics in Figures 4, 5, and 6.<sup>1</sup>

In Figure 4, we plot the pointwise mean and standard deviation of the large time solution of (13), (17)–(19) for different rates of gating,  $\alpha_0 + \alpha_1$ . In both plots, the markers (circles, plusses, and squares) are results of stochastic simulations of the random PDE. In the left plot, the curves are the analytical formula (43). In the right plot, the red curve is the analytical formula (33), which is valid for slow gating by Theorem 3.5. The right plot also verifies that the standard deviation vanishes for fast gating, as shown in section 4.1.2. In both plots, we take  $V = c_i = 1$  and  $\rho_0 = 1/2$ .

In Figure 5, we plot the pointwise mean and standard deviation of the large time solution of (13), (17)–(19) for different values of the potential,  $V$ . In both plots, the markers are the results of stochastic simulations of the random PDE. In

<sup>1</sup>The code used to generate the computational data is available on the GitHub database (<https://github.com/seanlawley>).

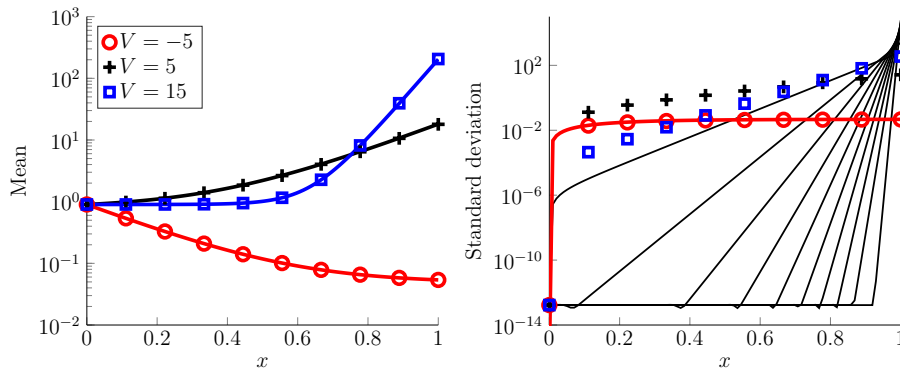


FIG. 5. Pointwise mean and standard deviation of the large time solution of (13), (17)–(19) for different values of the potential,  $V$ . The markers (circles, plusses, and squares) are the results of stochastic simulations. In the left plot, the curves are the analytical formula (43). In the right plot, the red curve is the analytical formula (33), which is valid for  $V \ll -1$  by Theorem 3.6. The thin black curves in the right plot are the results of stochastic simulations for  $V = 20, 40, \dots, 200$ , verifying that the standard deviation vanishes as  $V$  increases, as shown in Theorem 3.9. See section 4.2 for more details.

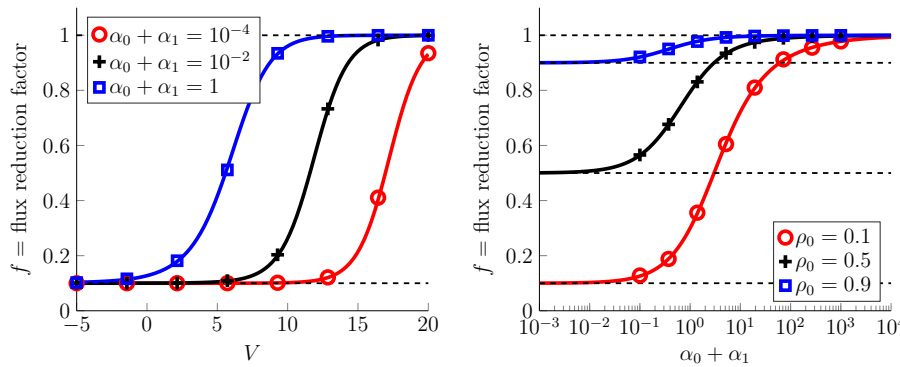


FIG. 6. How stochastic gating affects the mean flux through a channel. In both plots, the curves are the analytical formula (45). The markers (circles, plusses, and squares) are the results of stochastic simulations of the random PDE. See section 4.2 for more details.

the left plot, the curves are the analytical formula (43). In the right plot, the red curve is the analytical formula (33), which is valid for  $V \ll -1$  by Theorem 3.6. The thin black curves in the right plot are the results of stochastic simulations for  $V = 20, 40, \dots, 200$ , verifying that the standard deviation vanishes as  $V$  increases, as shown in Theorem 3.9. In both plots, we take  $c_1 = 0.9$ ,  $\rho_0 = 1/2$ , and  $\alpha_0 + \alpha_1 = 1$ .

In Figure 6, the curves are the analytical formula (45) for the factor  $f$  that relates the flux through a gated channel to the flux through a channel that is always open, (44). The markers are the results of stochastic simulations. In both plots, the top dashed black line is at 1, which is the limiting value of  $f$  for  $V \gg 1$  or  $\alpha_0 + \alpha_1 \gg 1$ . The lower black dashed lines are at  $\rho_0$ , which is the limiting value of  $f$  for  $V \ll -1$  or  $\alpha_0 + \alpha_1 \ll 1$ . In the left plot,  $\rho_0 = 0.1$ . In the right plot,  $V = 4$ .

**5. Physiological parameters.** It is commonly assumed that the flux through a gated channel,  $J_{\text{gated}}$ , is merely the flux through an always open channel,  $J_{\text{open}}$ ,

multiplied by the proportion of time open,  $\rho_0$ . That is,

$$(50) \quad J_{\text{gated}} \approx \rho_0 J_{\text{open}}.$$

Our model predicts that the flux through a gated channel is

$$(51) \quad J_{\text{gated}} = f J_{\text{open}},$$

where  $f \in (\rho_0, 1)$  is given in (45). We have shown that if the gating is sufficiently slow ( $\alpha_0 + \alpha_1 \ll 1$ ), then  $f \approx \rho_0$  and thus (50) is a good approximation. However, we have shown that if the gating is not slow, and/or the potential does not satisfy  $V \ll -1$ , then  $f$  can be much larger than  $\rho_0$  and, hence, (50) can significantly underestimate the flux through a gated channel. Indeed, if  $\rho_0$  is small and gating is fast and/or the potential is large, then (50) and (51) can differ by orders of magnitude.

Therefore, in this section we investigate the factor  $f$  as a function of physiologically reasonable parameter values. Since  $f$  depends on  $\alpha_0$ ,  $\alpha_1$ , and  $V$ , we need to estimate these three dimensionless parameters. We take the ion diffusion coefficient to be  $D_1 = 1 \times 10^{-9} \text{ m}^2/\text{s}$  [27], the channel length to be the thickness of a cell membrane,  $L = 10 \text{ nm}$  [23], the temperature to be  $293 \text{ K} = 20^\circ\text{C}$ , and a unit valence  $z = 1$ . Since potentials are generally in the range  $\bar{V} \in [-100, 100] \text{ mV}$  [14], it follows from (7) that the dimensionless potential is approximately in the range

$$(52) \quad V \in (-4, 4).$$

The time that a channel spends either open or closed can vary greatly [12], but unless the channel is bursting [6], it typically spends at least  $0.02 \text{ ms}$  in either state. Hence,  $\overline{\alpha_0} + \overline{\alpha_1}$  is typically no larger than  $100 \text{ ms}^{-1}$ , and thus

$$(53) \quad \alpha_0 + \alpha_1 \leq 0.01.$$

In Figure 6, we plot the factor  $f$  as a function of  $V$  for different choices of  $\alpha_0, \alpha_1$ . This figure shows that  $f \approx \rho_0$  for typical physiological parameters, and thus (50) is typically a good approximation. Interestingly though, this figure also shows that  $f$  is a steep sigmoidal function of  $V$ . In particular, if  $V$  is marginally outside the range in (52), then the approximation (50) breaks down. In addition, if there are circumstances in which  $\alpha_0 + \alpha_1$  surpasses the bound (53), then the approximation (50) rapidly breaks down for values of  $V$  in the physiological range (52).

**6. Discussion.** We have used mathematical modeling and analysis to investigate how stochastic gating affects the electrodiffusive flux through an ion channel. Our analysis predicts that

$$(54) \quad J_{\text{gated}} \approx \rho_0 J_{\text{open}} \quad \text{if } \alpha_0 + \alpha_1 \ll 1,$$

$$(55) \quad J_{\text{gated}} \approx \rho_0 J_{\text{open}} \quad \text{if } V \ll -1,$$

$$(56) \quad J_{\text{gated}} \approx J_{\text{open}} \quad \text{if } \alpha_0 + \alpha_1 \gg 1,$$

$$(57) \quad J_{\text{gated}} \approx J_{\text{open}} \quad \text{if } V \gg 1.$$

The result in (54) is intuitive. To see this, observe that there are four timescales in the problem. The first is the time it takes the ion concentration  $c(x, t)$  to relax to steady state when the gate is open ( $n \equiv 0$ ). Call this time  $\tau_0 = \tau_0(V, c_i)$ , noting that it depends only on the dimensionless parameters  $V$  and  $c_i$ . Similarly, let  $\tau_1 = \tau_1(V, c_i)$  be the time it takes  $c(x, t)$  to relax to steady state when the gate is closed ( $n \equiv 1$ ).

The other two timescales are the average time spent in the open state,  $1/\alpha_0$ , and the average time spent in the closed state,  $1/\alpha_1$ . For slow gating, we have that  $1/\alpha_0 + 1/\alpha_1 \gg \tau_0 + \tau_1$ , and thus the time spent transitioning between the open and closed steady states is negligible compared to the time spent in those steady states. Hence, for slow gating,  $c(x, t)$  becomes a two-state system that quickly switches between the open and closed steady states. Since the flux in the closed state is zero, the result (54) follows. While this explanation is intuitive, to our knowledge it has not been previously articulated. Furthermore, we have provided a precise quantitative description of what is “slow” gating in terms of only a few biophysical parameters in (44)–(45) above.

The results in (55), (56), and (57) require more mathematical analysis to understand intuitively. Roughly speaking, (55) follows from a similar argument as (54) after calculating that  $\tau_0 \rightarrow 0$  and  $\tau_1 \rightarrow 0$  as  $V \rightarrow -\infty$  (see Theorem 3.6 for the precise statement). The result in (57) is surprising, but it can be understood after finding that  $\tau_0 \rightarrow 0$  and  $\tau_1 \rightarrow \infty$  as  $V \rightarrow \infty$  (see Theorem 3.9 for the precise statement). The result in (56) is also surprising, and contrary to the other results, it cannot be understood solely in terms of the four timescales. Again, we emphasize that the transitions between the parameter regimes in (54)–(57) follow immediately from the analytical formula for  $J_{\text{gated}}$  in (44)–(45).

For typical physiological parameter values, we found that  $J_{\text{gated}} \approx \rho_0 J_{\text{open}}$ , which is often assumed in conductance-based neuron models. Interestingly though, we have found that  $J_{\text{gated}}$  can be much greater than  $\rho_0 J_{\text{open}}$  for parameters somewhat outside of typical physiological ranges.

Finally, while our model assumed a two-state channel for simplicity, more detailed gating models with multiple subunits of multiple types are more commonly used in the neurophysiology literature [5, 10, 14]. Our stochastic PDE model could be generalized to include a more complicated gating model, which would entail making the boundary conditions depend on a Markov chain with many states (rather than only two states). Though this generalization would certainly complicate the analysis, the model is likely still tractable, as analyzing PDEs with boundary conditions that switch between many states has been done in [17, 18, 20]. However, we predict that the various limiting behaviors of the gated flux given in (54)–(57) for the simple two-state model would still hold for these more detailed models (the parameter  $\alpha_0 + \alpha_1$  would simply be replaced by the analogous parameter describing the gating timescale of the more complicated model).

#### REFERENCES

- [1] A. M. BEREZHKOVSII AND S. M. BEZRUKOV, *Effect of stochastic gating on channel-facilitated transport of non-interacting and strongly repelling solutes*, J. Chem. Phys., 147 (2017), 084109.
- [2] A. M. BEREZHKOVSII AND S. Y. SHVARTSMAN, *Diffusive flux in a model of stochastically gated oxygen transport in insect respiration*, J. Chem. Phys., 144 (2016), 204101.
- [3] P. C. BRESSLOFF AND S. D. LAWLEY, *Moment equations for a piecewise deterministic PDE*, J. Phys. A, 48 (2015), 105001.
- [4] P. C. BRESSLOFF AND S. D. LAWLEY, *Stochastically gated diffusion-limited reactions for a small target in a bounded domain*, Phys. Rev. E (3), 92 (2015), 062117.
- [5] J. R. CLAY, *Excitability of the squid giant axon revisited*, J Neurophysiol., 80 (1998), pp. 903–913.
- [6] D. COLQUHOUN AND A. G. HAWKES, *On the stochastic properties of bursts of single ion channel openings and of clusters of bursts*, Philos. Trans. Roy. Soc. London Ser. B, 300 (1982), pp. 1–59.

- [7] H. CRAUEL, *Random point attractors versus random set attractors*, J. London Math. Soc. (2), 63 (2001), pp. 413–427.
- [8] C. R. DOERING, *Effect of boundary condition fluctuations on Smoluchowski reaction rates*, in Stochastic Processes in Physics, Chemistry, and Biology, Springer, Berlin, 2000, pp. 316–326.
- [9] G. B. ERMENTROUT AND D. H. TERMAN, *Mathematical Foundations of Neuroscience*, Springer New York, 2012.
- [10] J. H. GOLDWYN AND E. SHEA-BROWN, *The what and where of adding channel noise to the Hodgkin-Huxley equations*, PLOS Comput. Biol., 7 (2011), e1002247.
- [11] M. HÄUSSER, *The Hodgkin-Huxley theory of the action potential*, Nature Neurosci., 3 (2000), pp. 1165–1165.
- [12] B. HILLE, *Ion channels of excitable membranes*, Sinauer, Sunderland, MA, 2001.
- [13] A. L. HODGKIN AND A. F. HUXLEY, *A quantitative description of membrane current and its application to conduction and excitation in nerve*, J. Physiol., 117 (1952), pp. 500–544.
- [14] J. P. KEENER AND J. SNEYD, *Mathematical Physiology: I: Cellular Physiology*, Springer, New York, 2010.
- [15] S. D. LAWLEY, *Stochastic Switching in Evolution Equations*, PhD thesis, Duke University, Durham, NC, 2014.
- [16] S. D. LAWLEY, *Boundary value problems for statistics of diffusion in a randomly switching environment: PDE and SDE perspectives*, SIAM J. Appl. Dyn. Syst., 15 (2016), pp. 1410–1433.
- [17] S. D. LAWLEY, *A probabilistic analysis of volume transmission in the brain*, SIAM J. Appl. Math., 78 (2018), pp. 942–962.
- [18] S. D. LAWLEY, J. BEST, AND M. C. REED, *Neurotransmitter concentrations in the presence of neural switching in one dimension*, Discrete Contin. Dyn. Syst. Ser. B, 21 (2016), pp. 2255–2273.
- [19] S. D. LAWLEY, J. C. MATTINGLY, AND M. C. REED, *Stochastic switching in infinite dimensions with applications to random parabolic PDE*, SIAM J. Math. Anal., 47 (2015), pp. 3035–3063.
- [20] S. D. LAWLEY AND V. SHANKAR, *Asymptotic and Numerical Analysis of a Stochastic PDE Model of Volume Transmission*, preprint, <https://arxiv.org/abs/1812.11680>, 2018.
- [21] MATHWORKS, *MATLAB version 8.5.0.197613 (R2015a)*, Natick, MA, 2015.
- [22] J. C. MATTINGLY, *Ergodicity of 2D Navier-Stokes equations with random forcing and large viscosity*, Comm. Math. Phys., 206 (1999), pp. 273–288.
- [23] U. MORAN, R. PHILLIPS, AND R. MILO, *Snapshot: Key numbers in biology*, Cell, 141 (2010), pp. 1262–1262.
- [24] M. PICCOLINO, *Fifty years of the Hodgkin-Huxley era*, Trends in Neurosci., 25 (2002), pp. 552–553.
- [25] B. SCHMALFUSS, *A random fixed point theorem based on Lyapunov exponents*, Random Comput. Dynam., 4 (1996), pp. 257–268.
- [26] A. SZABO, D. SHOUP, S. H. NORTHRUP, AND J. A. MCCAMMON, *Stochastically gated diffusion-influenced reactions*, J. Chem. Phys, 77 (1982), pp. 4484–4493.
- [27] J. WANG, L. ZHANG, J. XUE, AND G. HU, *Ion diffusion coefficient measurements in nanochannels at various concentrations*, Biomicrofluidics, 8 (2014), 024118.